C_3-Symmetric Chiral Organolanthanide Complexes: Synthesis, Characterization, and Stereospecific Polymerization of α-Olefins[||]

Lenka Lukešová,[†] Benjamin D. Ward,[†,‡] Stéphane Bellemin-Laponnaz,[§] Hubert Wadepohl,[†] and Lutz H. Gade*[,†,‡]

Anorganisch-Chemisches Institut, Universität Heidelberg, Im Neuenheimer Feld 270, and Catalysis Research Laboratory (CaRLa), Im Neuenheimer Feld 584, 69120 Heidelberg, Germany, and Institut de Chimie, Université Louis Pasteur, Institut le Bel, 4 rue Blaise Pascal, 67000 Strasbourg, France

Received May 22, 2007

The trialkyl complexes [M(*i*Pr-trisox)($CH_2SiMe_2R)_3$] (R = Me, M = Y, (**1**), R = Ph, M = Lu (**2a**), R = Me, M = Lu (**2b**), Tm (**3**), Er (**4**), Ho (**5**), and Dy (**6**)) were prepared from 1,1,1-tris[(*S*)-4-isopropyloxazolinyl]ethane (*i*Pr-trisox) and the corresponding trialkyl precursors [$M(CH_2SiMe_2R)_3(THF)_n$]. Their molecular structures all display a highly distorted octahedral geometry, with the angles subtended at the metal center significantly deviating from the ideal 90°, which is attributed to the steric demands imposed by the large CH_2SiMe_2R ligands, both with each other and with the isopropyl groups of the *i*Pr-trisox ligand. Active catalysts for the polymerization of α-alkenes (*n*-hexene, *n*-heptene, and *n*-octene) were generated in situ by reaction of the trialkyl precatalyst with 2 equiv of trityl tetrakis(pentafluorophenyl)borate. In all cases polyolefins with M_w/M_n values of between 1.58 and 2.08 and isotacticities of 80−95% were obtained. The polymerization activity increases from lutetium to thulium and then subsequently decreases with increasing ionic radius of the metal due to a combination of activation with increasing ionic radius and decreasing catalyst stability.

Introduction

Cationic alkyl group 3 and lanthanide complexes have been extensively employed as catalysts for the polymerization of olefins.[1−4] While the chemistry of cyclopentadienyl-based complexes is well established,[5−12] there has been an increasing interest in recent years in the respective chemistry employing non-cyclopentadienyl ligands. The use of group 3 systems has been well studied in this regard, particularly in the past decade,[13−20] whereas the successful employment of lanthanide-based systems remains much less common.[21−23] One reason for this situation is related to the fact that lanthanide complexes can be difficult to characterize and are often much less thermally stable compared to their scandium and yttrium analogues. Consequently, many ligand systems are employed with group 3 metals but are rarely extended toward the lanthanide series. Despite this, however, there have been some recent examples of highly successful lanthanide catalysts for olefin polymerization.[14,15] These focused almost exclusively on ethylene as the monomer, while higher α-olefins have been less studied, particularly with respect to tacticity control in the polymer microstructure. A full understanding of the essential features governing a successful catalyst has not as yet been completely determined; however, it is becoming increasingly evident that the ionic radius of the metal plays an important role in many cases.[14]

[||] Dedicated to Prof. Gerard van Koten on the occasion of his 65th birthday.

* To whom correspondence should be addressed. Fax: +49-6221-545609. E-mail: lutz.gade@uni-hd.de.

[†] Universität Heidelberg.

[‡] CaRLa.

[§] Université Louis Pasteur.

(1) Gromada, J.; Carpentier, J. −F.; Mortreux, A. *Coord. Chem. Rev.* **2004**, *248*, 397.

(2) Arndt, S.; Okuda, J. *Adv. Synth. Catal.* **2005**, *347*, 339.

(3) Zeimentz, P. M.; Arndt, S.; Elvidge, B. R.; Okuda, J. *Chem. Rev.* **2006**, *106*, 2404.

(4) Hou, Z.; Wakatsuki, Y. *Coord. Chem. Rev.* **2002**, *231*, 1.

(5) Ballard, D. G. H.; Courtis, A.; Holton, J.; McMeeking, J.; Pearce, R. *J. Chem. Soc., Chem. Commun.* **1978**, 994.

(6) Burger, B. J.; Thompson, M. E.; Cotter, W. D.; Bercaw, J. E. *J. Am. Chem. Soc.* **1990**, *112*, 1566.

(7) Jeske, G.; Lauke, H.; Mauermann, H.; Swepston, P. N.; Schumann, H.; Marks, T. J. *J. Am. Chem. Soc.* **1985**, *107*, 8091.

(8) Jeske, G.; Schock, L. E.; Swepston, P. N.; Schumann, H.; Marks, T. J. *J. Am. Chem. Soc.* **1985**, *107*, 8103.

(9) Watson, P. L.; Parshall, G. W. *Acc. Chem. Res.* **1985**, *18*, 51.

(10) Shapiro, P. J.; Bunel, E.; Schaefer, W. P.; Bercaw, J. E. *Organometallics* **1990**, *9*, 867.

(11) Shapiro, P. J.; Cotter, W. D.; Schaefer, W. P.; Labinger, J. A.; Bercaw, J. E. *J. Am. Chem. Soc.* **1994**, *116*, 4623.

(12) (a) Hou, Z.; Zhang, Y.; Nishiura, M.; Wakatsuki, Y. *Organometallics* **2003**, *22*, 129. (b) Luo, Y.; Nishiura, M.; Hou, Z. *J. Organomet. Chem.* **2007**, *692*, 536. (c) Hou, Z.; Luo, Y.; Li, X. *J. Organomet. Chem.* **2006**, *691*, 3114. (d) Li, X.; Hou, Z. *Macromolecules* **2005**, *38*, 6767. (e) Li, X.; Baldamus, J.; Hou, Z. *Angew. Chem., Int. Ed.* **2005**, *44*, 962. (f) Luo, Y.; Baldamus, J.; Hou, Z. *J. Am. Chem. Soc.* **2004**, *126*, 13910.

(13) For reviews of the non-cyclopentadienyl chemistry of group 3 metals, see: (a) Piers, W. E.; Emslie, D. J. H. *Coord. Chem. Rev.* **2002**, *233/234*, 131. (b) Edelmann, F. T.; Freckmann, D. M. M.; Schumann, H. *Chem. Rev.* **2002**, *102*, 1851. (c) Mountford, P.; Ward, B. D. *Chem. Commun.* **2003**, 1797 and references therein.

(14) Bambirra, S.; Bouwkamp, M. W.; Meetsma, A.; Hessen, B. *J. Am. Chem. Soc.* **2004**, *126*, 9182.

(15) Arndt, S.; Spaniol, T. P.; Okuda, J. *Angew. Chem., Int. Ed.* **2003**, *42*, 5075.

(16) Luo, Y.; Baldamus, J.; Hou, Z. *J. Am. Chem. Soc.* **2004**, *126*, 13910.

(17) Banbirra, S.; van Leusen, D.; Meetsma, A.; Hessen, B.; Teuben, J. H. *Chem. Commun.* **2001**, 637.

(18) Long, D. P.; Bianconi, P. A. *J. Am. Chem. Soc.* **1996**, *118*, 12453.

(19) (a) Hajela, S.; Schaefer, W. P.; Bercaw, J. E. *J. Organomet. Chem.* **1997**, *532*, 45. (b) Lawrence, S. L.; Ward, B. D.; Dubberley, S. R.; Kozak, C. M.; Mountford, P. *Chem. Commun.* **2003**, 2880.

(20) Fryzuk, M. D.; Giesbrecht, G.; Rettig, S. J. *Organometallics* **1996**, *15*, 3329.

(21) Woodman, T. J.; Sarazin, Y.; Fink, G.; Hauschild, K.; Bochmann, M. *Macromolecules* **2005**, *38*, 3060.

(22) Collin, J.; Daran, J.-C.; Jacquet, O.; Schulz, E.; Trifonov, A. *Chem.—Eur. J.* **2005**, *11*, 3455.

(23) Trifonov, A.; Skvortsov, G. G.; Lyubov, D. M.; Skorodumova, N. A.; Fukin, G. K.; Baranov, E. V.; Glushakova, V. N. *Chem.—Eur. J.* **2006**, *12*, 5320.

10.1021/om700504f CCC: $37.00
Publication on Web 08/03/2007

Scheme 1. Synthesis of Complexes 1−6

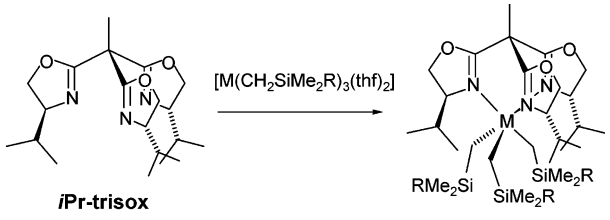

M	R	
Y	Me	**1**
Lu	Ph	**2a**
Lu	Me	**2b**
Tm	Me	**3**
Er	Me	**4**
Ho	Me	**5**
Dy	Me	**6**

In our laboratories we have embarked on an extensive research program focusing on the coordination chemistry and subsequent catalytic applications of the C_3-symmetric 1,1,1-tris(oxazolinyl)ethane ligand.[24−27] This ligand is ideally suited to the trivalent octahedral complexes commonly observed with lanthanides, since the symmetry and tripodal nature of the ligand render the remaining anionic coligands homotopic. In addition, the position of the chiral center on the ligand framework is such that the chiral information is efficiently transferred to the catalytically active site. We have recently reported on the use of the 1,1,1-tris[(*S*)-4-isopropyloxazolinyl]ethane (*i*Pr-trisox) ligand as a successful supporting environment for the scandium[28] and thulium[29] complexes [M(*i*Pr-trisox)(CH_2SiMe_3)$_3$], which proved to be precatalysts for the isospecific polymerization of α-olefins. The thulium complex was the first example of a *stereospecific* α-olefin polymerization catalyst based on a lanthanide. In due consideration of the importance of the ionic radius of the metal, we herein report on the preparation and catalytic activity of analogous complexes employing other lanthanides, to probe the generality of the system.

Results and Discussion

Synthesis and Structural Characterization of the *i*Pr-trisox/Trialkyl Complexes. Given the early results obtained with the scandium complex [Sc(*i*Pr-trisox)(CH_2SiMe_3)$_3$], we continued our investigations with yttrium and the lanthanides in order of increasing ionic radius. The syntheses of the [Ln(*i*Pr-trisox)(CH_2SiMe_3)$_3$] complexes were performed for metals ranging from lutetium to dysprosium (Scheme 1). Although we have previously demonstrated that the *i*Pr-trisox ligand will readily adapt to a wide range of ionic radii, we were unable to successfully prepare complexes with the lanthanides preceding dysprosium, possibly owing to the decreased stability of lanthanide alkyl complexes as the ionic radius increases. Interestingly, we were also unable to synthesize an ytterbium complex, which we attribute to redox side reactions.

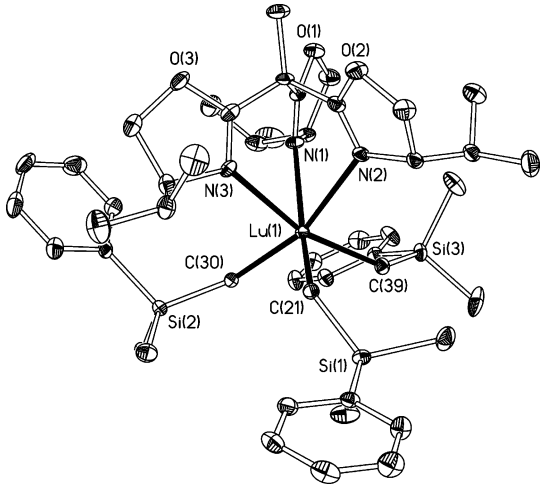

Figure 1. Molecular structure of [Lu(*i*Pr-trisox)(CH_2SiMe_2Ph)$_3$] (**2a**) (25% probability). Hydrogen atoms omitted for clarity. Selected bond lengths (Å) and angles (deg): C(21)−Lu(1), 2.379(4); C(30)−Lu(1), 2.373(4); C(39)−Lu(1), 2.372(4); Lu(1)−N(2), 2.504(3); Lu(1)−N(1), 2.510(3); Lu(1)−N(3), 2.522(3); C(39)−Lu(1)−C(30), 99.22(13); C(39)−Lu(1)−C(21), 99.24(14); C(30)−Lu(1)−C(21), 102.41(14); N(2)−Lu(1)−N(1), 71.84(11); N(2)−Lu(1)−N(3), 73.24(12); N(1)−Lu(1)−N(3), 73.81(11).

The trialkyl complexes [M(*i*Pr-trisox)(CH_2SiMe_2R)$_3$] (R = Me, M = Y (**1**), R = Ph, M = Lu (**2a**), R = Me, M = Lu (**2b**), Tm (**3**), Er (**4**), Ho (**5**), and Dy (**6**)) were prepared from the corresponding trialkyl precursors [M(CH_2SiMe_2R)$_3$(THF)$_n$] (Scheme 1). Although the trialkyl precursors for scandium and yttrium can be readily isolated, the corresponding complexes for the lanthanide metals are significantly less thermally stable. They were therefore synthesized at low temperature and used in situ. Subsequent to their preparation in pentane, the trialkyl complexes were reacted with the *i*Pr-trisox ligand, causing the immediate precipitation of the *i*Pr-trisox-supported complexes **1**−**6**. Thermal decomposition of these complexes was observed over a few days at ambient temperature, and thus, they were stored in the solid state at −40 °C.

The molecular structures of **2a,b**, **3**, **4**, **5**, and **6** were confirmed by X-ray diffraction. Diffraction-quality single crystals were grown from saturated dichloromethane solutions at −30 °C. The molecular structure of **2a** is shown in Figure 1 along with the principal bond lengths and angles. The crystals of the CH_2SiMe_3 derivatives **2b**, **3**, **4**, **5**, and **6** were isomorphous; the molecular structures of **5** and **6** are provided in Figures 2 and 3, with the principal bond lengths and angles listed in Table 1.

The structures all display a highly distorted octahedral geometry, with the angles subtended at the metal center significantly deviating from the ideal 90°. This is presumably due in part to the steric demands imposed by the large CH_2SiMe_2R ligands, both with each other and with the isopropyl groups of the *i*Pr-trisox ligand. This latter effect may also be invoked to explain the long M−N bonds. In contrast to the C−M−C angles of ca. 106° in **2b**, **3**, **4**, **5**, and **6**, the corresponding angles in **2a** are smaller, being 100−102°, presumably owing to the fact that the phenyl group, although larger, is rather flat and can be orientated in such a way as to minimize steric repulsion. The other essential structural features remain comparable to those of **2b**, **3**, **4**, **5**, and **6**. The mean M−N and M−C bond lengths in the structures of **2b**−**6** show a gradual increase with the effective ionic radius of the metal center, as illustrated in Figure 4.

The ^{1}H and ^{13}C NMR data of the yttrium and lutetium complexes **1**, **2a**, and **2b** are consistent with C_3-symmetric

(24) Bellemin-Laponnaz, S.; Gade, L. H. *Angew. Chem., Int. Ed.* **2002**, *41*, 3473.
(25) Dro, C.; Bellemin-Laponnaz, S.; Welter, R.; Gade, L. H. *Angew. Chem., Int. Ed.* **2004**, *43*, 4479.
(26) Bellemin-Laponnaz, S.; Gade, L. H. *Chem. Commun.* **2002**, 1286.
(27) (a) Gade, L. H.; Marconi, G.; Dro, C.; Ward, B. D.; Poyatos, M.; Bellemin-Laponnaz, S.; Wadepohl, H.; Sorace, L.; Poneti, G. *Chem.−Eur. J.* **2007**, *13*, 3058. (b) Foltz, C.; Enders, M.; Bellemin-Laponnaz, S.; Wadepohl, H.; Gade, L. H. *Chem.−Eur. J.* **2007**, *13*, 5994.
(28) Ward, B. D.; Bellemin-Laponnaz, S.; Gade, L. H. *Angew. Chem., Int. Ed.* **2005**, *44*, 1668.
(29) Lukešová, L.; Ward, B. D.; Bellemin-Laponnaz, S.; Wadepohl, H.; Gade, L. H. *Dalton Trans.* **2007**, 920.

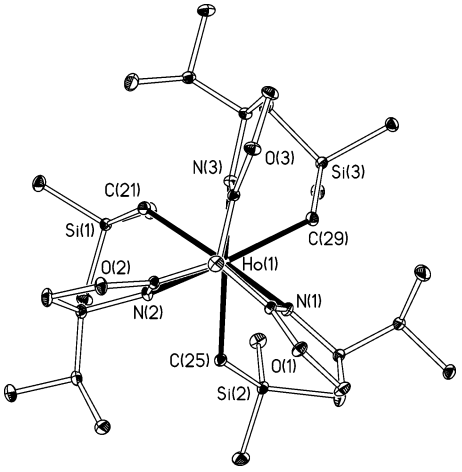

Figure 2. Molecular structure of [Ho(*i*Pr-trisox)(CH_2SiMe_3)$_3$] (**5**) (25% probability). Hydrogen atoms omitted for clarity.

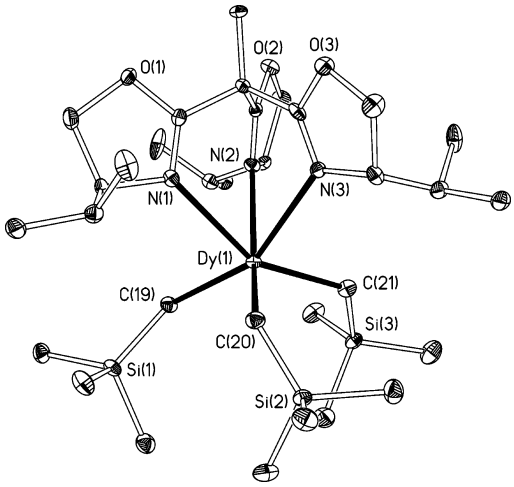

Figure 3. Molecular structure of [Dy(*i*Pr-trisox)(CH_2SiMe_3)$_3$] (**6**) (25% probability). Hydrogen atoms omitted for clarity.

structures, with only a single set of resonances being observed for the oxazolines and alkyl ligands, at both 295 and 215 K. This suggests that the N_3-bound coordination of the *i*Pr-trisox ligand observed in the solid state pertains in solution. The paramagnetic ^{1}H NMR spectra were recorded for complexes **3**−**6**. Although the spectra could not be unambiguously assigned, all spectra display sharp resonances between +160 and −220 ppm, with resonance patterns that are consistent with the C_3-symmetric structures observed in the solid state, as well as in the NMR spectra of the diamagnetic complexes.

Polymerization of *n*-Hexene, *n*-Heptene, and *n*-Octene. We have previously reported that the scandium and thulium trialkyl

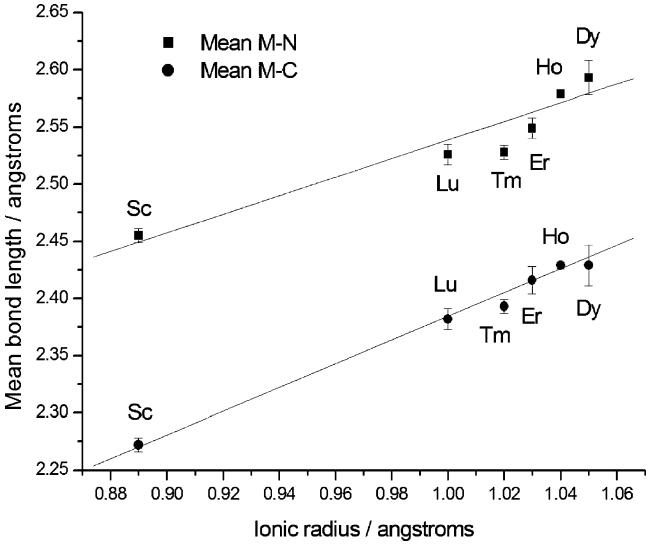

Figure 4. Effective ionic radii vs the mean M−N and M−C bond lengths in the molecular structures of **2b**−**6**.

Scheme 2. Isotactic Polymerization of 1-Hexene, 1-Heptene, and 1-Octene

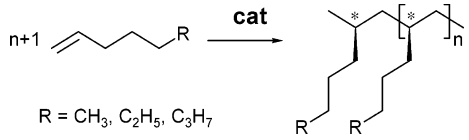

complexes supported by the *i*Pr-trisox ligand are active olefin polymerization catalysts for α-alkenes when activated with 2 equiv of trityl tetrakis(pentafluorophenyl)borate.[28,29] We found that the phenyl dimethyl derivative **2a** showed no polymerization activity at all, which we attribute to the cationic species being unstable. This was verified by NMR tube scale experiments between **2a** and [Ph_3C][$B(C_6F_5)_4$], in which only a complex mixture of products was obtained. Consequently, we confined our studies to the trimethyl congeners **2b**−**6**. The active catalysts were generated in situ by reaction of the trialkyl precatalyst with 2 equiv of activator in chlorobenzene. Under these conditions very poor activities were observed, which we attribute to thermal decomposition of the cationic species. The decomposition was circumvented by carrying out the activation process at −5 °C before immediately adding the appropriate olefin and maintaining the temperature at −5 °C for the duration of the reaction (15 min for 1-hexene and 1-heptene, 30 min for 1-octene). Under these conditions *n*-hexene, *n*-heptene, and *n*-octene were polymerized (Scheme 2). Reducing the reaction time afforded correspondingly less polymer, suggesting that the catalysts retain at least some activity for the total duration of the reaction. In all cases polyolefins with M_w/M_n values of

Table 1. Selected Bond Lengths (Å) and Angles (deg) for [M(*i*Pr-trisox)(CH_2SiMe_3)$_3$] (M = Lu (2b), Er (4), Ho (5), Dy (6))

	Sc[a]	**2b** (Lu)[b]	Tm[29]	**4** (Er)	**5** (Ho)	**6** (Dy)
M−N(1)	2.456(2)	2.519(2)	2.557(3)	2.536(3)	2.5646(9)	2.600(5)
M−N(2)	2.446(1)	2.532(3)	2.565(3)	2.550(3)	2.5792(9)	2.580(4)
M−N(3)	2.464(2)	2.527(2)	2.542(3)	2.562(3)	2.5929(10)	2.600(5)
M−C(21)	2.270(2)	2.388(3)	2.394(4)	2.415(4)	2.4304(12)	2.432(6)
M−C(25)	2.272(2)	2.375(3)	2.393(4)	2.405(4)	2.4284(12)	2.432(6)
M−C(29)	2.275(2)	2.384(3)	2.395(4)	2.428(3)	2.4295(12)	2.423(6)
N(1)−M−N(2)	74.90(5)	72.11(9)	71.55(10)	72.23(13)	71.96(3)	70.70(18)
N(1)−M−N(3)	73.95(5)	73.03(9)	72.58(11)	71.81(13)	71.11(3)	70.72(16)
N(2)−M−N(3)	73.81(5)	71.84(8)	71.75(11)	71.65(11)	71.11(3)	71.74(18)
C(21)−M−C(25)	106.69(7)	106.18(11)	106.69(14)	108.03(13)	107.94(4)	107.2(2)
C(21)−M−C(29)	104.38(7)	107.50(10)	108.47(13)	106.85(13)	106.73(4)	106.6(2)
C(25)−M−C(29)	105.51(8)	105.93(11)	106.64(14)	105.75(13)	106.33(5)	108.0(2)

[a] From ref 28. Equivalent bond lengths and angles are listed, although the actual numbering scheme in ref 28 differs slightly from that of the structures reported herein. [b] From ref 29.

Table 2. Polymerization Activities for [M(*i*Pr-trisox)(CH_2SiMe_3)$_3$] When Activated with 2 equiv of [Ph_3C][$B(C_6F_5)_4$]

Ln	R^d (Å)	monomer	activity[a]	M_w/M_n	M_n[b]	M_w[b]	isotacticity[c]
Lu	1.00	1-hexene	137	1.65	0.901	1.49	88
Lu		1-heptene	74.2	1.91	1.19	2.26	89
Lu		1-octene	38.9	1.69	1.64	2.78	80
Tm[e]	1.02	1-hexene	165	1.95	1.26	2.46	90
Tm[e]	1.02	1-heptene	120	2.08	0.99	2.06	83
Tm[e]	1.02	1-octene	30	1.80	1.18	2.13	95
Er	1.03	1-hexene	122	1.62	1.02	1.65	80
Er		1-heptene	49.4	2.01	1.03	2.08	80
Er		1-octene	31.4	1.65	1.02	1.69	90
Ho	1.04	1-hexene	65.8	1.69	0.818	1.38	85
Ho		1-heptene	33.3	1.95	0.561	1.10	80
Ho		1-octene	30.9	1.90	0.778	1.48	80
Dy	1.05	1-hexene	66	1.58	0.675	1.07	85
Dy		1-heptene	48.4	1.61	0.551	0.888	80
Dy		1-octene	28.9	1.58	0.722	1.14	80

[a] Units of kg mol^{-1} h^{-1}. [b] Units of 10^5 g mol^{-1}. [c] Percentage of *mmmm* pentad in the $^{13}C\{^1H\}$ NMR spectrum. [d] Effective ionic radius of Ln^{3+} for CN = 6; see ref 36. [e] See ref 29.

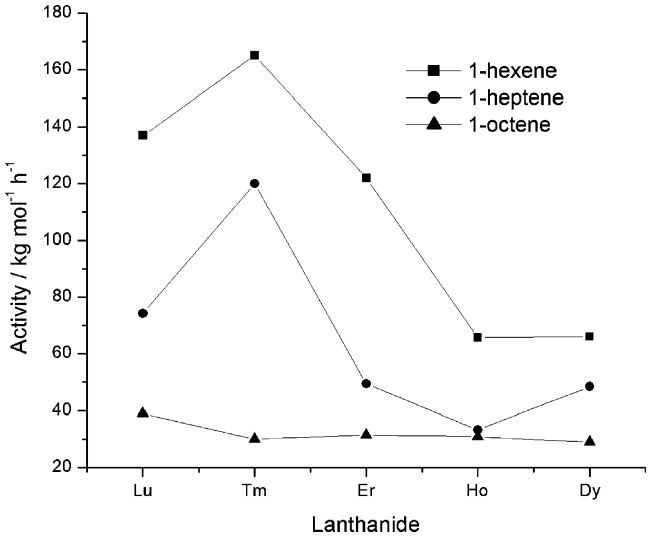

Figure 5. Olefin polymerization data for [M(*i*Pr-trisox)(CH_2SiMe_3)$_3$] (M = Lu, Tm, Er, Ho, and Dy).

between 1.58 and 2.08 and isotacticities of 80−95% determined by ^{13}C NMR spectroscopy (vide infra) were obtained. The polymerization data are summarized in Table 2 and are illustrated in Figure 5.[28,29]

Interestingly, the polymerization activity increases from lutetium to thulium[29] and then subsequently decreases with increasing ionic radius of the metal, which at first seems to be contrary to the observation made by Okuda, who reports an increase of activity with the larger metals.[15] We attribute the activity trend in this case to two effects, the first being that the activity increases with ionic radius owing to the greater space (and potentially higher coordination number) around the larger metals and the second being the decreased stability of the active species as the size of the metal increases, a phenomenon supported by our observation that the stability of the trialkyl precatalysts in the solid state also decreases for the larger lanthanides. This explanation follows the observations on amidinate complexes made by Hessen, who reports a steady increase of activity with increasing ionic radius, reaching a maximum at yttrium, followed by a decrease in activity as the stability of the complex decreases.[14] For the trisox-supported yttrium complex, only traces (<10 mg) of polymer were formed under these conditions. Although the above explanation is consistent with the polymerization activities observed with the lanthanide metals, we note that none of the activities are

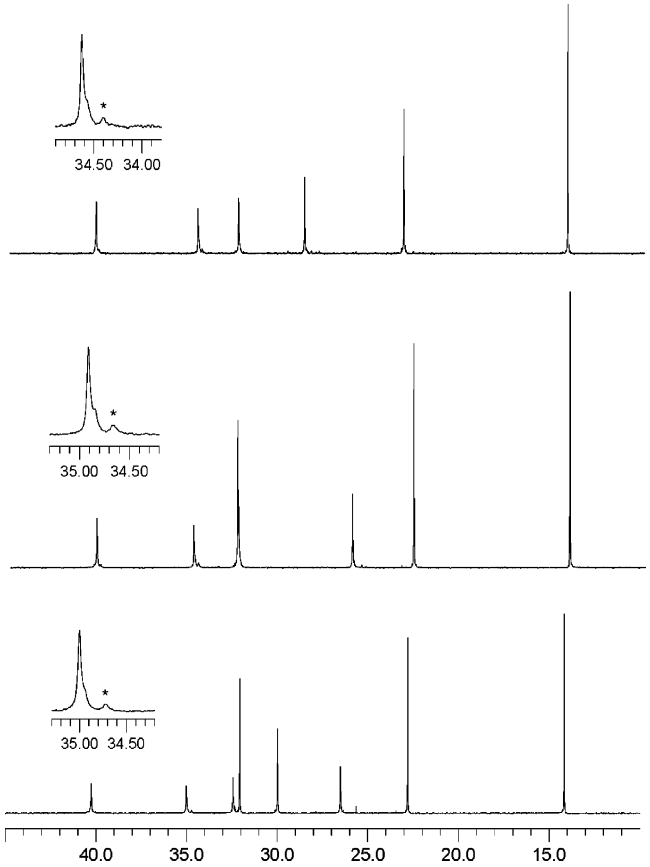

Figure 6. $^{13}C\{^1H\}$ NMR spectra of 1-hexene (top), 1-heptene (middle), and 1-octene (bottom). Resonances marked with an asterisk in the expansions correspond to the *mmmr* pentad, the first pentad to be observed downfield of the *mmmm* pentad.[30]

comparable to those observed with the scandium congener [Sc(*i*Pr-trisox)(CH_2SiMe_3)$_3$], which was found to polymerize 1-hexene with an activity of 36000 kg mol^{-1} h^{-1} at ambient temperature.[28]

For each catalyst the polymerization activity was observed to decrease in the order 1-hexene > 1-heptene > 1-octene, which is consistent with the increased steric demands imposed by the longer alkyl chain of the olefin. This difference in the activity was much more pronounced between 1-hexene and 1-heptene, whereas the difference was less pronounced for 1-heptene and 1-octene. The polymerization activities for 1-octene were relatively constant at around 30−40 kg mol^{-1} h^{-1}. The M_w values of the polymers were found to be in the range of 88800−278000 g mol^{-1}, with generally higher molecular weights being obtained with the smaller lanthanides lutetium and thulium. The lower values for the larger metals are possibly attributed to the lower stability of the catalysts based on metals with larger ionic radii (vide supra).

In each case, the stereocontrol in the polymer microstructure was determined by integration of the resonance in the $^{13}C\{^1H\}$ NMR spectra corresponding to the *mmmm* pentad in the C3 carbon resonance at ca. 35 ppm.[30] A representative example of a $^{13}C\{^1H\}$ NMR spectrum for each of the polymers obtained with the lutetium catalyst **2a** is provided in Figure 6. In each case good to excellent tacticity control was observed, regardless of the metal and monomer in question, being between 80% and 95% isotactic. Such consistent control is indicative of the efficient transmission of the chiral information from the trisox ligand to the catalytically active site on the metal center. This

(30) Asakura, T.; Demura, M.; Nishiyama, Y. *Macromolecules* **1991**, *24*, 2334.

is also illustrative of the ligand's ability to readily adapt to the changing environment of different metal sizes and to maintain efficient stereocontrol under such varying conditions.

Conclusion

We have illustrated that the *i*Pr-trisox ligand is a highly suitable supporting environment for a range of group 3 and lanthanide metals up to an ionic radius of 1.05 Å (Dy). As observed previously by others,[2,3,14] the activity of the lanthanide-based polymerization catalysts depends on the ionic radius of the metal. However, none of the trisox−lanthanide systems display a catalytic activity which is comparable to that of the scandium catalyst reported previously by us.

The C_3-symmetric environment is very efficient at transmitting the chiral information to the catalytic site in stereoselective olefin polymerization, with a remarkable degree of tacticity control being observed for a range of α-olefins.

Experimental Section

General Information. All manipulations were performed under an inert atmosphere of dry argon using standard Schlenk techniques or by working in a glovebox. Solvents were dried over potassium (thf), sodium/potassium alloy (pentane), or CaH_2 (dichloromethane), distilled, and thoroughly degassed prior to use. Deuterated solvents were dried over potassium (C_6D_6) or CaH_2 (CD_2Cl_2), vacuum distilled, and stored in Teflon valve ampules under argon. ^1H and $^{13}C\{^1H\}$ NMR spectra were recorded on Bruker Avance 200, 400, and 600 NMR spectrometers and were referenced using the residual proton solvent peak (^1H) or carbon resonance (^{13}C). Elemental analyses were recorded by the analytical service of the Heidelberg Chemistry Department. $Y(CH_2SiMe_3)_3(thf)_2$ was prepared according to published procedures.[31] All other reagents were obtained from commercial sources and used as received unless explicitly stated. The microanalyses of complexes **1**, **2b**, **5**, and **6** were persistently and consistently low in carbon, despite repeated recrystallization. This is attributed to carbide formation and incomplete combustion, which is a common observation with group 3 and lanthanide complexes containing metal−carbon bonds.[32]

General Procedure for [M(CH$_2$SiMe$_3$)$_3$(*i*Pr-trisox)] (M = Lu, Ho, Dy). Anhydrous lanthanide trichloride (1.82 mmol) was slurried in THF (30 mL) and stirred overnight. The THF was removed under reduced pressure and the solid suspended in pentane (20 mL). The resulting suspension was cooled to −80 °C for the dropwise addition of a cooled (−10 °C) solution of $LiCH_2SiMe_3$ (512.2 mg, 5.4 mmol) in pentane (40 mL). The mixture was stirred at −10 °C for 2 h. The reaction was filtered, and to the resulting solution was added a cooled (−78 °C) solution of *i*Pr-trisox (327 mg, 0.9 mmol) in pentane (50 mL), which caused precipitation of the product, which was isolated by filtration and dried in vacuo at room temperature. The crude product was extracted with CH_2Cl_2 (40 mL) and filtered. The solution was concentrated to 20 mL and cooled to −30 °C overnight to yield the pure product as a crystalline solid.

[Y(*i*Pr-trisox)(CH$_2$SiMe$_3$)$_3$] (1). To a cooled solution of $Y(CH_2SiMe_3)_3(THF)_2$ (177 mg, 0.358 mmol) in pentane (20 mL) at 0 °C was added a solution of *i*Pr-trisox (130 mg, 0.358 mmol) in pentane (10 mL). A white precipitate was formed immediately, and the reaction was stirred for 30 min before the supernatant solution was decanted. The precipitate was washed with pentane (2 × 10 mL) and dried in vacuo to afford [Y(*i*Pr-iPr-trisox)(CH_2SiMe_3)$_3$]. Yield: 126 mg (49%). ^1H NMR (399.9 MHz, CD_2Cl_2, 293 K): δ 4.58 (3 H, ddd, C*H*iPr, ^3J = 9.7 Hz, ^3J = 5.5 Hz, ^3J = 3.5 Hz), 4.43 (3 H, dd, C*H*HO, ^2J = 9.1 Hz, ^3J = 5.6 Hz), 4.32 (3 H, app t, CH*H*O, app J = 9.9 Hz), 2.38 (3 H, d sept, C*H*Me$_2$, ^3J = 6.9 Hz, ^3J = 3.4 Hz), 1.71 (3 H, s, Me$_{apical}$), 0.89 9 H, d, CH*Me*$_2$, ^3J = 7.1 Hz), 0.65 (9 H, d, CH*Me*$_2$, ^3J = 6.8 Hz), 0.04 (27 H, s, SiMe$_3$), −0.93 (6 H, d, C*H*$_2$SiMe$_3$, ^2J(YH) = 2.7 Hz) ppm. $^{13}C\{^1H\}$ NMR (100.6 MHz, CD_2Cl_2, 293 K): δ 167.8 (C═N), 71.1 (CH_2O), 70.9 (*C*H*i*Pr), 43.9 (*C*Me$_{apical}$), 33.7 (*C*H$_2$SiMe$_3$, ^1J(YC) = 33.5 Hz), 29.5 (*C*HMe$_2$), 18.7 (CH*Me*$_2$), 14.2 (CH*Me*$_2$), 14.5 (Me$_{apical}$), 4.6 (SiMe$_3$) ppm. $^{29}Si\{^1H\}$ NMR (CD_2Cl_2, 39.7 MHz, 293 K): −4.5 (SiMe$_3$) ppm. Anal. Found (Calcd) for $C_{32}H_{66}N_3O_3Si_3M$: C, 53.1 (53.8); H, 9.2 (9.3); N, 5.8 (5.9).

Data for [Lu(*i*Pr-trisox)(CH$_2$SiMe$_2$Ph)$_3$] (2a). White crystalline solid. Yield: 64%. ^1H NMR (399.9 MHz, C_6D_6, 293 K): δ 7.94 (6 H, d, *o*-C_6H_5, ^3J = 6.5 Hz), 7.33 (6 H, t, *m*-C_6H_5 ^3J = 7.3 Hz), 7.20 (3 H, t, *p*-C_6H_5, ^3J = 7.3 Hz), 4.32 (3 H, m, C*H*iPr), 3.62 (3 H, dd, C*H*HO, ^2J = 9.2 Hz, ^3J = 5.3 Hz), 3.33 (3 H, app t, CH*H*O, app J = 9.5 Hz), 2.45 (3 H, d sept, C*H*Me$_2$, ^3J = 6.8 Hz, ^3J = 3.3 Hz), 1.49 (3 H, s, Me$_{apical}$), 0.92 (3 H, d, LuCH$_2$, ^2J = 6.7 Hz), 0.81 (3 H, d, LuCH$_2$, ^2J = 6.8 Hz), 0.75 (9 H, s, SiMe), 0.72 (9 H, s, SiMe), 0.44 (9 H, overlapping d, CH*Me*$_2$, ^3J = 6.7 Hz) ppm. $^{13}C\{^1H\}$ NMR (100.6 MHz, C_6D_6, 293 K): 167.8 (C═N), 164.9 (*ipso*-C_6H_5), 148.8 (C_6H_5), 134.2 (C_6H_5), 128.3 (C_6H_5) 70.8 (CH_2O), 70.6 (*C*H*i*Pr), 43.7 (*C*Me$_{apical}$), 37.3 (CH*Me*$_2$), 29.2 (*C*HMe$_2$), 18.2 (CH*Me*$_2$), 14.0 (Me$_{apical}$), 4.4 (SiMe), 3.3 (SiMe), not observed (*C*H$_2$-SiMe$_3$) ppm.

Data for [Lu(*i*Pr-trisox)(CH$_2$SiMe$_3$)$_3$] (2b). White crystalline solid. Yield: 39%. ^1H NMR (399.9 MHz, CD_2Cl_2, 293 K): δ 4.52 (3 H, m, C*H*iPr), 4.43 (3 H, dd, C*H*HO, ^2J = 9.0 Hz, ^3J = 5.3 Hz), 4.30 (3 H, app t, CH*H*O, app J = 9.6 Hz), 2.40 (3 H, d sept, C*H*Me$_2$, ^3J = 6.9 Hz, ^3J = 3.5 Hz), 1.72 (3 H, s, Me$_{apical}$), 0.88 (9 H, d, CH*Me*$_2$, ^3J = 7.1 Hz), 0.65 (9 H, d, CH*Me*$_2$, ^3J = 6.8 Hz), −0.04 (27 H, s, SiMe$_3$), −0.39 (6 H, overlapping d, C*H*$_2$SiMe$_3$, ^2J = 10.9 Hz) ppm. $^{13}C\{^1H\}$ NMR (100.6 MHz, CD_2Cl_2, 293 K): δ 166.8 (C═N), 71.2 (CH_2O), 71.1 (*C*H*i*Pr), 43.6 (*C*Me$_{apical}$), 29.3 (*C*HMe$_2$), 18.7 (CH*Me*$_2$), 14.8 (Me$_{apical}$), 14.3 (CH*Me*$_2$), 4.2 (SiMe$_3$), not observed (*C*H$_2$SiMe$_3$) ppm. $^{29}Si\{^1H\}$ NMR (CD_2Cl_2, 39.7 MHz, 293 K): −4.9 (SiMe$_3$) ppm. Anal. Found (Calcd) for $C_{32}H_{66}N_3O_3Si_3M$: C, 47.4 (48.0); H, 8.2 (8.3); N, 5.2 (5.3).

[Er(*i*Pr-trisox)(CH$_2$SiMe$_3$)$_3$] (4). Anhydrous erbium trichloride (1.82 mmol) was slurried in THF (30 mL) and stirred overnight. The THF suspension was cooled to −78 °C for the dropwise addition of a cooled (−78 °C) solution of $LiCH_2SiMe_3$ (512.2 mg, 5.4 mmol) in pentane (40 mL). The reaction was warmed to −20 °C and stirred until all the solids had dissolved (ca. 20 min) before removal of the volatiles under reduced pressure. The reaction was extracted with toluene (30 mL) at −10 °C, and to the resulting solution was added a cooled (−78 °C) solution of *i*Pr-trisox (327 mg, 0.9 mmol) in pentane (50 mL). The resulting solution was then concentrated to approximately 2 mL, and the product was precipitated by the addition of pentane (50 mL). The product was isolated by filtration and dried in vacuo at room temperature. The crude product was extracted with CH_2Cl_2 (40 mL) and filtered. The solution was concentrated to 20 mL and cooled to −30 °C overnight to yield the pure product as a crystalline solid. Pink crystalline solid. Yield: 58%. ^1H NMR (399.9 MHz, CD_2Cl_2, 293 K): δ 94.00, 69.95, 12.95, 7.77, −10.16, −33.31, −39.21, −46.85, −132.18, −143.53 ppm. Anal. Found (Calcd) for $C_{32}H_{66}N_3O_3Si_3M$: C, 48.3 (48.5); H, 8.2 (8.4); N, 5.1 (5.3).

Data for [Ho(*i*Pr-trisox)(CH$_2$SiMe$_3$)$_3$] (5). Pale pink crystalline solid. Yield: 48%. ^1H NMR (499.9 MHz, CD_2Cl_2, 293 K): δ 87.70, 84.25, 20.81, 15.72, 14.47, 6.30, 2.65, −2.76, −12.94, −53.04 ppm. Anal. Found (Calcd) for $C_{32}H_{66}N_3O_3Si_3M$: C, 47.7 (48.6); H, 8.3 (8.4); N, 5.1 (5.3).

Data for [Dy(*i*Pr-trisox)(CH$_2$SiMe$_3$)$_3$] (6). White crystalline solid. Yield: 65%. ^1H NMR (399.9 MHz, CD_2Cl_2, 293 K): δ 205.76, 192.33, 47.81, 27.70, 19.42, 14.79, −0.75, −12.37, −26.77,

(31) Lappert, M. F.; Pearce, R. *J. Chem. Soc., Chem. Commun.* **1973**, 126.

(32) For example, see: Ward, B. D.; Dubberley, S. R.; Maisse-François, A.; Gade, L. H.; Mountford, P. *Dalton Trans.* **2002**, 4649.

Table 3. X-ray Data for Compounds 2a, 2b, 4, 5, and 6

	2a	2b	4	5	6
empirical formula	$C_{47}H_{72}LuN_3O_3Si_3$	$C_{32}H_{66}LuN_3O_3Si_3$	$C_{32}H_{66}ErN_3O_3Si_3$	$C_{32}H_{66}HoN_3O_3Si_3$	$C_{32}H_{66}DyN_3O_3Si_3$
fw	986.32	800.12	792.41	790.08	787.65
cryst size/mm	0.35 × 0.15 × 0.15	0.25 × 0.20 × 0.20	0.15 × 0.15 × 0.10	0.25 × 0.25 × 0.10	0.15 × 0.10 × 0.10
cryst syst	orthorhombic	monoclinic	monoclinic	monoclinic	monoclinic
space group	$P2_12_12_1$	$P2_1$	$P2_1$	$P2_1$	$P2_1$
a/Å	11.202(2)	10.2048(10)	10.2557(6)	10.2711(2)	10.3013(14)
b/Å	20.432(4)	19.115(2)	19.0994(11)	19.1776(3)	19.200(3)
c/Å	22.582(5)	10.3849(10)	10.3659(6)	10.4005(2)	10.4282(14)
α/deg	90	90	90	90	90
β/deg	90	102.054(2)	102.011(1)	101.947(1)	102.000(3)
γ/deg	90	90	90	90	90
V/Å^3	5168.9(18)	1981.0(3)	1986.0(2)	2004.26(6)	2017.5(5)
Z	4	2	2	2	2
D_c/Mg m^{-3}	1.267	1.341	1.325	1.309	1.297
μ/mm^{-1}	2.018	2.614	2.235	2.095	1.972
max, min transm	0.7517, 0.5386	0.59, 0.52	0.7460, 0.5598	0.4596, 0.3569	0.4294, 0.2545
index ranges, *hkl*	−14 to +14, 0 to +26, 0 to +29	−15 to +14, −28 to +28, 0 to +15	−13 to +13, −25 to +25, 0 to +13	−20 to +20, −39 to +39, 0 to +21	−13 to +13, −25 to +25, 0 to +14
θ/deg	1.8−27.5	2.0−32.1	2.0−28.3	2.0−46.5	2.0−28.7
T/K	193(2)	173(2)	173(2)	100(2)	150(2)
F(000)	2048	832	826	824	822
no. of reflns collected	127115	13330	41782	269587	16058
no. of independent reflns [R_{int}]	11846 [0.1026]	13302 [0.0462]	9856 [0.0588]	35569 [0.0612]	10286 [0.0614]
no. of data/restraints/params	11846/0/527	12143/1/380	9856/37/395	35569/1/411	10286/1/395
GOF on F^2	1.058	1.0563	1.066	1.064	0.992
final *R* indices [$I > 2\sigma(I)$]	R1 = 0.039, wR2 = 0.60	R1 = 0.030, wR2 = 0.034	R1 = 0.032, wR2 = 0.065	R1 = 0.026, wR2 = 0.058	R = 0.049, wR2 = 0.107
R indices (all data)	R1 = 0.046, wR2 = 0.062	R1 = 0.034, wR2 = 0.352	R1 = 0.041, wR2 = 0.068	R1 = 0.031, wR2 = 0.060	R = 0.062, wR2 = 0.112
absolute structure param	−0.012(5)	0.001(5)	−0.011(7)	−0.001(3)	−0.037(11)
largest residual peak/e Å^{-3}	1.413 and −0.663	3.81 and −2.76	0.846 and −0.928	3.649 and −1.296	1.541 and −0.629

−126.35 ppm. Anal. Found (Calcd) for $C_{32}H_{66}N_3O_3Si_3M$: C, 48.2 (48.8); H, 8.3 (8.5); N, 5.3 (5.3).

Polymerization Studies. A 20 μmol sample of the catalyst **1a** was dissolved in chlorobenzene (1 mL) and added to trityl tetrakis(pentafluorophenyl)borate (40 μmol) at −5 °C. The appropriate α-olefin (1 mL) was added, and the mixture was stirred for a given period of time. At the end of the reaction, methanol (5 mL) was added to quench the catalyst, and the volatiles were removed under reduced pressure to yield the polyolefin as a waxy solid. The $^{13}C\{^1H\}$ NMR spectra of the polyolefins are provided in the Supporting Information.

Crystal Structure Determinations. Suitable crystals of **2a**, **2b**, **3**, **4**, **5**, and **6** were obtained from saturated solutions in dichloromethane at −20 °C. Intensity data were collected at low temperature on a Bruker Smart 1000 CCD (**3**, **4**, **5**, **6**) or an Enraf-Nonius Kappa-CCD diffractometer (**2a,2b**). The structures were solved using heavy atom or direct methods, with absorption corrections being applied as part of the data scaling procedure. After refinement of the heavy atoms, difference Fourier maps revealed the maxima of residual electron density close to the positions expected for the hydrogen atoms. They were introduced as fixed contributors in the structure factor calculations and treated with a riding model with isotropic temperature factors but not refined. A final difference map revealed no significant maxima of residual electron density. Structure solution and refinement were performed by using the programs SHELXS-86,[33] SHELXL-97,[34] CRYSTALS,[35] and (DIRDIF).[36] Crystal data and experimental details are provided in Table 3.

Acknowledgment. We thank the Deutsche Forschungsgemeinschaft (Grant SFB 623 and postdoctoral fellowship to L.L.), the EU (Marie Curie EIF fellowship to B.D.W.), BASF AG, the state of Baden-Württemberg, and the University of Heidelberg (postdoctoral fellowship to B.D.W. within CaRLa) for financial support.

Supporting Information Available: CIF files giving crystal data for compounds **2a**, **2b**, and **4**−**6**. This material is available free of charge via the Internet at http://pubs.acs.org.

OM700504F

(33) Sheldrick, G. M. *SHELXS-86*; University of Göttingen: Göttingen, Germany, 1986.

(34) Sheldrick, G. M. *SHELXL-97*; University of Göttingen: Göttingen, Germany, 1997.

(35) Watkin, D. J.; Prout, C. K.; Carruthers, J. R.; Betteridge, P. W.; Cooper, R. I. *CRYSTALS*, issue 11; Chemical Crystallography Laboratory: Oxford, U.K., 2001.

(36) Beurskens, P. T.; Beurskens, G.; de Gelder, R.; Garcia-Granda, S.; Gould, R. O.; Israel, R.; Smits, J. M. M. DIRDIF-99, University of Nijmegen, The Netherlands, 1999.